

THIS FILE IS MADE AVAILABLE THROUGH THE DECLASSIFICATION EFFORTS AND RESEARCH OF:

THE BLACK VAULT

THE BLACK VAULT IS THE LARGEST ONLINE FREEDOM OF INFORMATION ACT / GOVERNMENT RECORD CLEARING HOUSE IN THE WORLD. THE RESEARCH EFFORTS HERE ARE RESPONSIBLE FOR THE DECLASSIFICATION OF THOUSANDS OF DOCUMENTS THROUGHOUT THE U.S. GOVERNMENT, AND ALL CAN BE DOWNLOADED BY VISITING:

[HTTP://WWW.BLACKVAULT.COM](http://www.blackvault.com)

YOU ARE ENCOURAGED TO FORWARD THIS DOCUMENT TO YOUR FRIENDS, BUT PLEASE KEEP THIS IDENTIFYING IMAGE AT THE TOP OF THE .PDF SO OTHERS CAN DOWNLOAD MORE!



DEPARTMENT OF THE AIR FORCE

30TH SPACE WING (AFSPC)

26 May 98

30 CS/SCBR
867 Washington Ave.
Vandenberg AFB CA 93437-6120


John Greenewald, Jr.
[REDACTED]

Dear Mr. Greenewald

Reference your Freedom of Information Act (FOIA) request of 9 May 98 (30 CS #98-124) for a copy of report number 97-350/5.2-01, Cassini Hazards to RTG Study. Under the Freedom of Information Act, we are releasing the requested information.

Any questions or concerns regarding this matter, you can contact myself at (805) 734-8232 x6-7006.

Sincerely


GEORGINA S. SANDERS, SrA, USAF
Freedom of Information Act Manager

Cassini Hazards to RTG Study (Revised)

ACTA

Distribution authorized to US Government agencies and their contractors to protect administrative/operational use data,
31 July 1997. Other requests for this document shall be referred to the 30th Space Wing (AFSPC) Safety Office
(30 SW/SE), Vandenberg AFB, CA 93437 or 45th Space Wing (AFSPC) Safety Office (45 SW/SE), Patrick AFB, FL
32925.

Technical Report No. 97-350/5.2-01

CASSINI HAZARDS TO RTG STUDY
(Revised)

Contract No. FO4684-97-C-0001
Task No. 5

Prepared for

Department of the Air Force
30th Space Wing (AFSPC)
Vandenberg AFB, CA 93437

and

Department of the Air Force
45th Space Wing (AFSPC)
Patrick AFB, FL 32925

Prepared by

Steven L. Carbon

ACTA

2790 Skypark Dr., Suite 310
Torrance, CA 90505-5345

July 1997

REPORT DOCUMENTATION PAGE

Form Approved
OMB No. 074-0188

Public reporting burden for this collection of information is estimated to average 1 hour per response, including the time for reviewing instructions, searching existing data sources, gathering and maintaining the data needed, and completing and reviewing this collection of information. Send comments regarding this burden estimate or any other aspect of this collection of information, including suggestions for reducing this burden to Washington Headquarters Services, Directorate for Information Operations and Reports, 1215 Jefferson Davis Highway, Suite 1204, Arlington, VA 22202-4302, and to the Office of Management and Budget, Paperwork Reduction Project (0704-0188), Washington, DC 20503.

1. AGENCY USE ONLY (Leave blank)		2. REPORT DATE 31 July 1997	3. REPORT TYPE AND DATES COVERED Final 1 Oct 1996 - 30 Sep 1997	
4. TITLE AND SUBTITLE Cassini Hazards to RTG Study (Revised)			5. FUNDING NUMBERS C: FO4684-97-C-0001 TA: 5	
6. AUTHOR(S) Steven L. Carbon				
7. PERFORMING ORGANIZATION NAME(S) AND ADDRESS(ES) ACTA Inc. 2790 Skypark Dr., Suite 310 Torrance, CA 90505-5345			8. PERFORMING ORGANIZATION REPORT NUMBER 97-350/5.2-01	
9. SPONSORING / MONITORING AGENCY NAME(S) AND ADDRESS(ES) Department of the Air Force 30th Space Wing and 45th Space Wing Safety Office Safety Office Vandenberg AFB, CA 93437 Patrick AFB, FL 32925			10. SPONSORING / MONITORING AGENCY REPORT NUMBER	
11. SUPPLEMENTARY NOTES				
12a. DISTRIBUTION / AVAILABILITY STATEMENT Distribution authorized to U.S. Government agencies and their contractors to protect administrative/operational use data, 31 July 1997. Other requests for this document shall be referred to 30th Space Wing (AFSPC) Safety Office (30 SW/SE), Vandenberg AFB, CA 93437 or 45th Space Wing (AFSPC) Safety Office (45 SW/SE), Patrick AFB, FL 32925.				12b. DISTRIBUTION CODE
13. ABSTRACT (Maximum 200 Words) In this report we discuss the nuclear related hazards that may arise from the launch of the Cassini spacecraft to Saturn, scheduled in late 1997 aboard a Titan IVB vehicle. The energy sources of the Cassini are contained in three Radioisotope Thermoelectric Generators (RTGs). Each RTG contains 72 plutonium clad pellets. A hazard may be created if an RTG is damaged and the clad exposed. First, we examine the result of the malfunction tumble turn in the first ten seconds of flight, which may lead to intact impact of the full vehicle. Employing a Monte Carlo simulation, we estimate the relative probability between tail and nose impacts. Since the RTGs are near the nose, the latter case could lead to severe RTG damage if stuck by the vehicle stack. We then consider an on-trajectory thrust termination destruction. Here, we compute the probability for a solid propellant fragment to impact on an RTG. Statistics are also kept on the average number of fragments that impact near the RTG, the danger now being the combined heat from the burning fragments.				
14. SUBJECT TERMS Cassini, RTG, Impact study			15. NUMBER OF PAGES 33	16. PRICE CODE
17. SECURITY CLASSIFICATION OF REPORT UNCLASSIFIED	18. SECURITY CLASSIFICATION OF THIS PAGE UNCLASSIFIED	19. SECURITY CLASSIFICATION OF ABSTRACT UNCLASSIFIED	20. LIMITATION OF ABSTRACT SAR	

TABLE OF CONTENTS

Section	Page
1. INTRODUCTION	1
2. MALFUNCTION TUMBLE TURN METHODOLOGY	2
2.1 Tumble Turn Simulation	2
2.2 Torque Distribution	4
2.3 Inertial and Aerodynamic Breakup Model	5
2.4 Command Destruct Model	5
2.5 Explosion Velocity Model	7
2.6 Vehicle Impact Model	10
3. SUMMARY OF RESULTS	13
3.1 Intact Vehicle Impacts	13
3.2 Hazard Due to Propellant Explosion Pressure	17
3.3 Hazard Due to Heat Transfer	23
4. REFERENCES	28

LIST OF FIGURES

Figure	Page
2-1 Thrust Offset in Tumble Turn Plane	2
2-2 MFCO Reaction Model - Nominal	6
2-3 MFCO Reaction Model - Upper Estimate	7
3-1 Titan IVB SRMU Failure Mode Tree	19

LIST OF TABLES

Table		Page
2-1	Torque Distribution Functions	4
2-2	Selected Mean Explosion Speeds	8
2-3	Titan Pad Geometry	12
3-1	Initial Nose vs. Tail Results	14
3-2	Final Nose vs. Tail Results	15
3-3	Intact Vehicle Statistics	15
3-4	Nominal MFCO Model Impact Speed Histogram	16
3-5	Upper Estimate MFCO Model Impact Speed Histogram	17
3-6	Probabilities of RTG Struck by Propellant for Thrust Termination	22
3-7	Probabilities of RTG Struck by Propellant for Tumble Turns	23
3-8	Average Number of Fragment Impacts near RTG for Thrust Termination	25
3-9	Average Number of Fragment Impacts near Modules for Thrust Termination	25
3-10	Average Number of Fragment Impacts near RTG for Tumble Turns	26
3-11	Average Number of Fragment Impacts near Modules for Tumble Turns	26
3-12	Probabilities of RTG Coincident With Propellant for Thrust Termination	27
3-13	Probabilities of RTG Coincident With Propellant for Tumble Turns	27

1. INTRODUCTION

The second mission of the Titan IVB launch vehicle will be the Cassini spacecraft to Saturn. Due to the energy and vehicle requirements and of the vehicle, it contains three Radioisotope Thermoelectric Generators (RTGs). A Cassini RTG Safety analysis is currently being pursued by several investigators to evaluate the associated launch area nuclear risks in the event of a malfunction. This report discusses two analyses performed by ACTA to support the Safety Office at the 45th Space Wing. The main focus is to determine the probability that an RTG will be struck on the ground by solid propellant. Results are also obtained when, at vehicle breakup, the RTGs are broken into their eighteen module components.

The first task is to determine the relative probability that an intact vehicle, which experiences a malfunction tumble turn (MFT), will impact the ground nose down. This would force the RTGs to impact first and suffer a direct strike by the full stack of the vehicle. This is of greatest concern in the first 10 to 15 seconds of flight, during which time the vehicle may strike either concrete or sand. The number of full stack intact impacts is attenuated by accounting for vehicle breakup due to inertial loads, and command destruct (CD) due to action by the Mission Flight Control Officer (MFCO). If the vehicle is destroyed prior to impact, it is assumed that the Auto-Destruct System (ADS) is 100 percent effective. Thus, for MFT events, either the full stack impacts or total destruct occurs.

The second task examines the possible outcomes if the vehicle breaks up in flight due to an on-trajectory thrust termination (TT). In contrast to an MFT event, a TT event may disable the ADS leading to a partial vehicle destruct in which large segments of the Solid Rocket Motor Upgrades (SRMUs) are not destroyed. Here, the main interest is the probability that an SRMU solid propellant fragment strikes an RTG or its module components.

Although the central problem involves direct RTG strikes by solid propellant, there is a residual danger due to heat transfer from a nearby burning propellant fragment to the RTG or module. The concern is that given sufficient heat energy, the interior nuclear clads may become exposed and create a nuclear hazard. The requisite heat can either be due to a large SRMU segment, or several smaller solid propellant fragments contributing heat. To evaluate this hazard for both MFT and TT events, we compute the average number of solid propellant fragments that will impact within a specified distance of the RTG or module.

2. MALFUNCTION TUMBLE TURN METHODOLOGY

A computer program called RTGSIM was coded to perform the detailed analysis outlined in the introduction. In this section, we present the algorithms employed for this purpose. Much of the code was extracted from the Simulated Explosion program, SIMEX [1].

2.1 Tumble Turn Simulation

To simulate the tumble turn, consider the geometry of Figure 2-1 where F is the thrust force and d is the distance from the vehicle's center of gravity to the tail of the SRMU segments. The orientation of the y axis with respect to the ground is specified by the roll angle, which is randomly selected uniformly from 0 to 360°. At $t=0$ the vehicle roll axis is directed along the positive x axis. The thrust force is applied at the pivot joint of the SRMUs, which is shown as the aft end of the rocket in the figure (where the nozzles are not shown). The dynamics are defined by the torque equation

$$\tau(t) = \bar{F}(t) \times \bar{d}(t) = F(t) d(t) \sin \psi = I(t) \frac{d^2}{dt^2} \theta(t) \quad (2-1)$$

where $I(t)$ is the moment of inertia. Since most vehicles are not cylindrical, the value of $I(t)$ depends on orientation of the tumble turn plane. Examination of the Titan IV data book [2] shows that, to within a few percent error, $I_{xx} \approx I_{yy}$. Even as the solid propellant burns, this relation holds up since

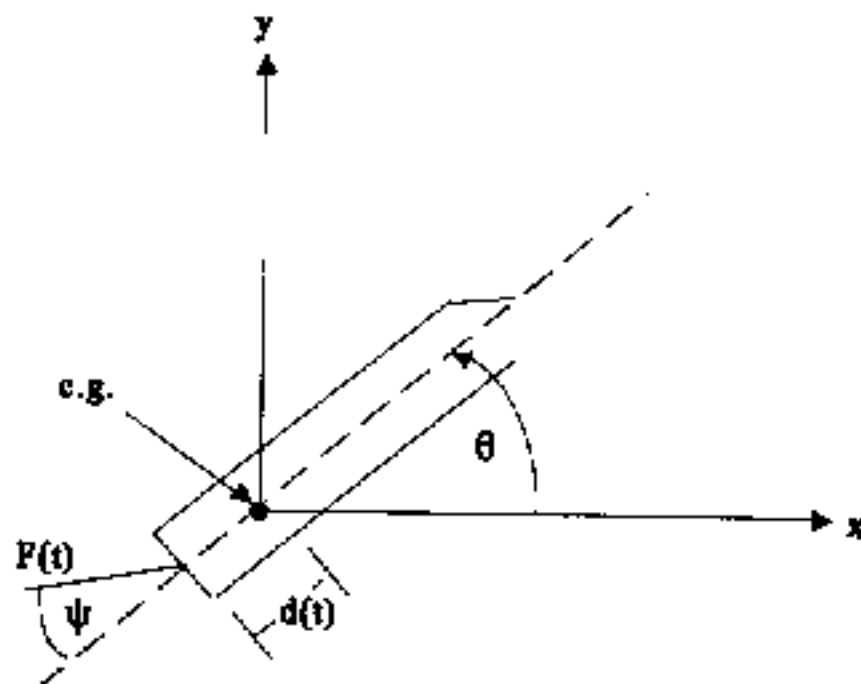


Figure 2-1. Thrust Offset in Tumble Turn Plane

inside the SRMU's the propellant burns radially outward from the center. Integrating twice gives an expression for the total angle of rotation,

$$\theta(t) = \int_0^t \int_0^{t_1} \frac{F(t_1) d(t_1) \sin \psi}{2I(t_1)} dt_2 dt_1 \quad (2-2)$$

where $F(t)$, $d(t)$ and $I(t)$ are obtained from table lookup.

To construct the equations of motion, we need the components of the thrust force in the tumble turn plane. For $\theta=0$, trigonometry gives

$$\begin{aligned} F_x &= F \cos \psi \\ F_y &= -F \sin \psi \end{aligned} \quad (2-3)$$

For general rotation angles, we apply the standard coordinate transformation

$$\begin{pmatrix} F_x \\ F_y \end{pmatrix} = \begin{pmatrix} \cos \theta & -\sin \theta \\ \sin \theta & \cos \theta \end{pmatrix} \begin{pmatrix} F \cos \psi \\ -F \sin \psi \end{pmatrix} \quad (2-4)$$

The equations of motion $\vec{F} = m \vec{a}$, where m is the total mass of the vehicle and a is net acceleration, reduce to the component form

$$\begin{aligned} \frac{d^2 x}{dt^2} &= \frac{F(t) \cos \psi}{m(t)} \cos \theta(t) + \frac{F(t) \sin \psi}{m(t)} \sin \theta(t) \\ \frac{d^2 y}{dt^2} &= \frac{F(t) \cos \psi}{m(t)} \sin \theta(t) - \frac{F(t) \sin \psi}{m(t)} \cos \theta(t) \end{aligned} \quad (2-5)$$

We obtain the velocity as a function of time by integrating,

$$\begin{aligned} v_x(t) &= v_0 + \cos \psi \int_0^t \frac{F(t)}{m(t)} \cos \theta(t) dt + \sin \psi \int_0^t \frac{F(t)}{m(t)} \sin \theta(t) dt \\ v_y(t) &= \cos \psi \int_0^t \frac{F(t)}{m(t)} \sin \theta(t) dt - \sin \psi \int_0^t \frac{F(t)}{m(t)} \cos \theta(t) dt \end{aligned} \quad (2-6)$$

where v_0 is the magnitude of the nominal state velocity at the start of the tumble turn. Integrating again yields the position of the vehicle's center of gravity. The tumble turn plane is subsequently rotated about the x axis to account for the roll angle.

2.2 Torque Distributions

The malfunction tumble turn is governed by the nozzle (gimbal) deflection. RTGSIM initiates the turn by randomly selecting the gimbal offset angle, ψ . Physically, for the Titan IVB, this angle can span $-7^\circ < \psi < +7^\circ$. The nozzle deflection results from an applied torque associated with some Basic Initiating Event (BIE)¹. Since torque is directly proportional to the gimbal deflection angle, the latter can be obtained using a torque distribution function.

By determining the most likely BIEs, Lockheed-Martin generated the time dependent function shown in Table 2-1 [3]. These distributions reflect known malfunction initiating events and their relative probabilities. When plotted they produce an approximate "bathtub" shape, with the smallest torques dominating the distribution.

Table 2-1. Torque Distribution Functions

Time Span	Normalized Torque				
	0.0-0.2	0.2-0.4	0.4-0.6	0.6-0.8	0.8-1.0
0-10 sec	0.6154	0.0891	0.0891	0.0891	0.1173
10-30sec	0.5865	0.0940	0.0940	0.0940	0.1315

The bathtub distribution has a drawback in that it is not very conservative. The table shows that about 60 percent of the deflection angles will be less than $0.2 \times 7.0^\circ = 1.4^\circ$. Tumble turns initiated with such small nozzle deflections experience a relatively long flight time until impact. In practice, it is found that during this time and under these conditions there is an overwhelming chance the vehicle will experience either inertial breakup or command destruct. On the other hand, the intact vehicle impacts are driven by hard-over turns, which correspond to large torque. For the bathtub distribution, the hard-over case occurs in about 10 percent of the simulations.

¹ The L-M term used to describe failure events that eventually lead to AOC's (Accident Outcome Events).

Due to the amount of uncertainty and guesswork that was involved in the L-M study (*i.e.*, determining the BIEs, assigning their probabilities and torques, *etc.*), many of the RTGSIM runs were performed with a uniform torque distribution. This distribution is more conservative than the bathtub distribution in that the hard over nozzle event is twice as likely to occur. Not unexpectedly, the number of intact vehicle impacts is also approximately twice as large.

2.3 Inertial and Aerodynamic Breakup Model

Inertial and aerodynamic breakup reflects the structural tolerance of the vehicle. Breakup follows when the inertial load exceeds the physical limitations of some critical portion of the vehicle. To try to force a complete destruction, the Titan IVB has sensors that activate the ADS when the vehicle begins to breakup. The ADS is designed to prevent free-flying SRMU's and an incomplete destruction of the vehicle. In this study, it is assumed that the ADS is completely reliable.

The inertial breakup model for the Titan IVB employed by SIMEX was generated by Lockheed-Martin. An explicit expression was obtained which relates the mean inertial breakup time \bar{t} to the thrust offset torque τ :

$$\bar{t} = 127.66 - 16.21 \log_{10}(\tau) \quad (2-7)$$

where the time is measured from the start of the tumble turn. The time is in units of seconds and the units of torque are in ft-lbs. The time to inertial breakup, t , is then uniformly selected from the interval $(0.2\bar{t}, 2.0\bar{t})$.

Vehicle breakup, and subsequent ADS activation may also result from excessive aerodynamic forces. Since drag is not implicitly modeled in RTGSIM, the program triggers the ADS if vehicle speed exceeds 650 feet per second during a tumble turn.

2.4 Command Destruct Model

Although there is no consensus in the MFCO community on a generic command destruct reaction model, the "Mike Frank" model has been used for the Cassini mission [4]. This model was obtained by consolidating empirical data coupled with a particular cognitive model. It assumes that, in the first few seconds of flight, action will be taken if the vehicle experiences obviously erratic flight. To assist the MFCO in detecting such a flight, there will be a Vehicle Attitude Display present and laser tracking of the vehicle. To ensure the proper environment for laser tracking, the mission rules

will only allow the launch to proceed if there is total visibility for the laser light to travel unobstructed through the atmosphere.

The response time curve for nominal conditions is shown in Figure 2-2. Here, the elapsed time is measured from when the vehicle axis is first offset 45° from its nominal orientation. We also assume a probability of failure of the Flight Termination System (FTS) system. For our analysis, we have been directed to use 0.00018. Since there may be circumstances that prevent the MFCO from performing at optimal levels, a modification of this model has further been developed [5]. This model, shown in Figure 2-3, represents an upper 3 σ estimate of the reaction time, and is clearly more conservative than the nominal case. This second model accounts for effects such as lack of visual clarity, eye movement and adjustment, and interruption due to additional information inputs. Associated with this model, is the more conservative FTS failure probability of 0.0018.

Vehicle destruct as a result of receiving a CD signal initiated by the MFCO generally produces the same outcome as an ADS event. However, in this case, there is an acknowledged small probability that initiating CD does not always produce a response. A breakdown of the Flight Termination System FTS may prevent the signal from ever being sent. When the FTS fails, the vehicle may still self destruct if there is sufficient time for the inertial and aerodynamic load forces to reach criticality. In the worst case, FTS failure may lead to an intact impact for vehicle malfunctions that occur very early after liftoff (before ten seconds).

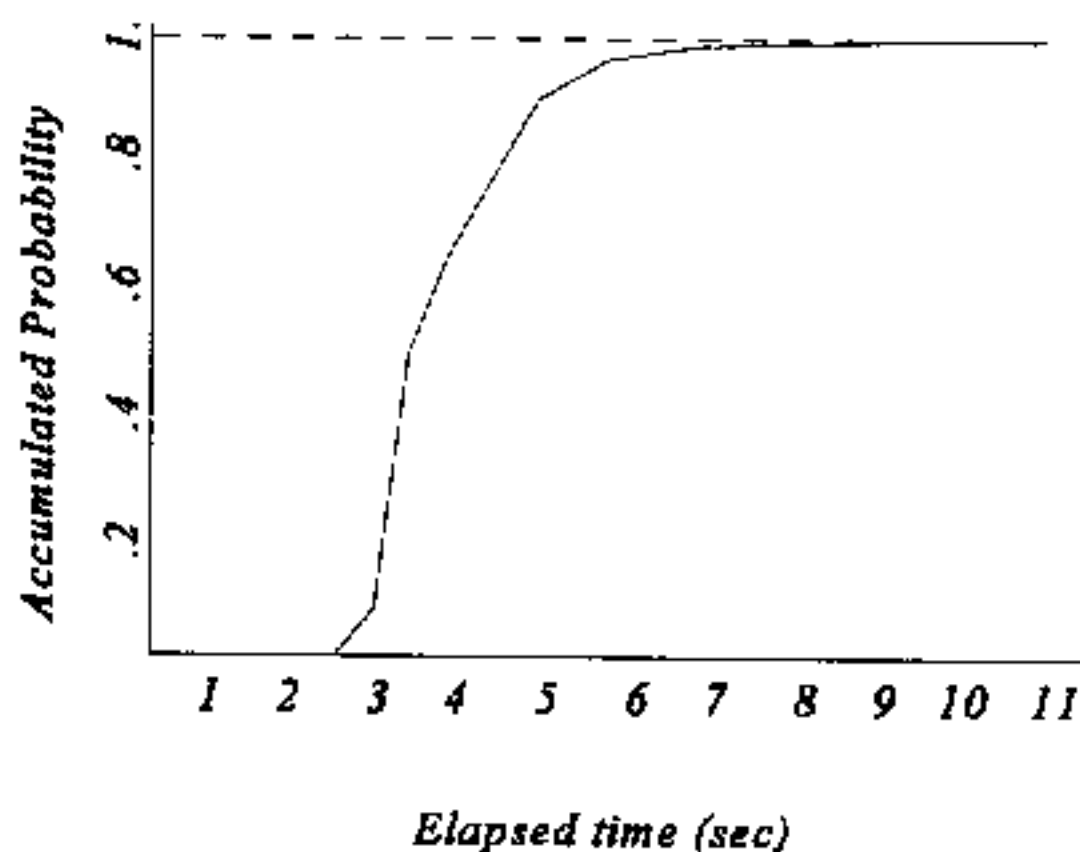


Figure 2-2. MFCO Reaction Model - Nominal

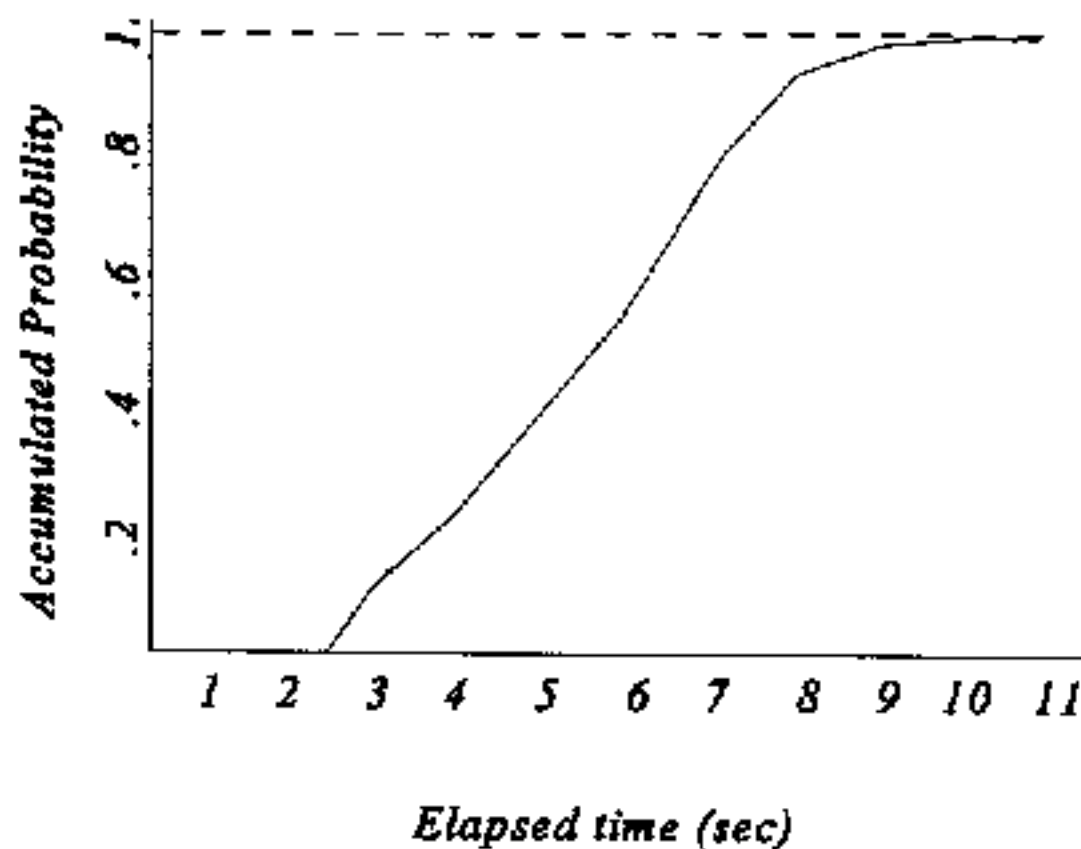


Figure 2-3. MFCO Reaction Model - Upper Estimate

2.5 Explosion Velocity Model

When breakup occurs, most fragments receive an induced velocity. Here, we will ignore inert debris fragments from the Titan IVB since our concern involves the interaction of the RTGs with solid propellant. The direction distribution and magnitude of the induced explosion velocity vector depends on the fragment type and its initial location on the vehicle. We identify three separate categories of fragments: (1) intact RTGs attached to the Cassini spacecraft or exposed module components, (2) solid propellant fragments from a completely destroyed SRMU, and (3) intact SRMU segments. Our treatment of these cases is extracted from several other sources, except one additional case introduced in this study. We now discuss separately the models for the explosion speeds and the directions.

Explosion Speed

The explosion speeds, v , are assumed to obey a normal distribution, $\eta(\bar{v}, \sigma_v)$, with probability density function

$$p(v) = \frac{1}{\sqrt{2\pi}\sigma_v} e^{-\frac{1}{2} \frac{(v-\bar{v})^2}{\sigma_v^2}} \quad (2-8)$$

where \bar{v} is the mean explosion speed, and σ_v is the one-sigma explosion speed uncertainty. To relate the mean and uncertainty we further assume that the normalized distribution is given by $\eta(1,0.3)$. These values can then be obtained from the upper three-sigma value, z , measured from zero velocity. Thus, by definition,

$$z = \bar{v} + 3\sigma_v \quad (2-9)$$

Using our distribution, $\sigma_v = 0.3\bar{v}$, and so

$$\bar{v} = \frac{z}{1.9} \quad (2-10)$$

In Table 2-2 we explicitly give the time independent mean explosion speeds. The reference numbers in the second column indicate the source of the corresponding speed uncertainty values. The first two rows indicate that relatively small values are used for the Cassini spacecraft with the RTGs attached and the modules components of a destructed RTG. These values were obtained by rescaling the values used by L-M by one third for an 80 ms ignition delay time [8].

Table 2-2. Selected Mean Explosion Speeds

Component	Mean Explosion Speed
Cassini Spacecraft (with RTGs)	4.2 ft/sec
RTG modules	10.5 ft/sec
Forward segment assembly	31.6 ft/sec
Center segment	0 ft/sec [7]
Aft segment assembly	0 ft/sec [7]
Nozzle	0 ft/sec [7]
Dome	time dependent [8]
Solid Propellant Fragments	time dependent [8]

The explosion speed of large intact SRMU segments is essentially zero due to their large inertia. Yet, for the forward assembly and the dome, Table 2-2 indicates that rather larger speeds have been assigned. This is an attempt to account for the residual thrust of these segments, which is difficult

to model directly. The thrust is directed out of the broken end of the segment since the dome prevents any escape in the other direction. The residual thrust for the forward assembly, in the third row of the table, was obtained by trial and error using RTGSIM. This value was able to reproduce the Titan 34 D9 forward segment intact piece range as a one and a half sigma event. By contrast, the original values given in [7] for the forward assembly were considered to be unreasonably large.

There is no net thrust for the center, aft assembly, or nozzle segments even though burning solid propellant still exists. For the center segment, the thrust forces from the ends cancel since the bore holes are the same diameters. For the aft assembly or nozzle, the forces balance when the bore hole is the same diameter as the nozzle exhaust throat. This configuration is approximately maintained in the first ten to fifteen seconds of flight, which is the same time span of interest for this study.

Explosion Direction

The Cassini spacecraft resides just below the nose of the vehicle. The shock due to destruction will cause the spacecraft, either with intact RTGs or broken into module components, to be ejected primarily along the longitudinal axis of the Titan vehicle [9]. In particular, we assume that an ejected piece is confined to a 40° cone, centered on the longitudinal axis. Transverse to this axis, the explosion directions obey a normal distribution where the extremes of the cone represent three-sigma events. Around the longitudinal axis, the directions are uniformly distributed.

The SRMU solid propellant fragments are assumed to be ejected primarily transverse to the vehicles' axis [9]. The explosion directions of the fragments fan out into a 40° wedge, with a normal distribution whose center is along the transverse axis. As above, the edges of the fan correspond to three-sigma events.

Finally, the forward assembly and the dome are considered to eject in directions represented by a uniform distribution over a hemisphere. The center of this hemisphere is pierced by the longitudinal axis of the vehicle. The random deviate, z , which selects the angle, is obtained from

$$z = \sin^{-1} x \quad (2-11)$$

where x is a uniform random deviate in the interval $[0,1]$. Note that in [9] the forward segment was given zero explosion velocity, which is unrealistic since they do not model the residue thrust. The distribution given here is unique to RTGSIM.

2.6 Vehicle Impact Model

The most hazardous outcome of a MFT event is impact of the full intact stack. With the focus on the risks to the RTGs, not all intact impacts are of the same degree of danger. Factors that influence the impact hazard are orientation of the vehicle, impact speed, and surface hardness. However, before these can be discussed, it is first necessary to clearly state when vehicle "impact" occurs. The RTGSDM code propagates the center of gravity (cg) point of the vehicle through the tumble turn. However, testing for cg impact would underestimate the number of intact vehicle impacts. This is because during the time when the first point on the vehicle actually strikes the ground and later when cg impact occurs, there may be either an ADS or CD action taken. When we discuss our results, we will quantify the importance of this consideration.

The relevant impacts are those that lead to an explosion of the solid propellant, or ground impact of the RTGs. In the reference frame of the vehicle, the tumble turn motion is seen as a rotation about its center of mass. Thus, the vehicle will generally first strike the ground at either its nose or tail, and has a very small chance of side-on impact. Since the Cassini spacecraft resides within the payload fairing, our study focused on the relative number of nose impacts. The uppermost section of the payload fairing is constructed of a thin metal dome, which will easily break away from the rest of the vehicle on impact without consequences. Therefore, we ignore the top thirty one feet of the vehicle when testing for nose impact. Similarly, if the nozzles strike the ground, they will detach from the SRMUs without affecting the solid propellant within the motors. Thus, since these nozzles are ten feet in length, this distance is also ignored when testing for SRMU tail impacts.

To track the location of the vehicle's nose and tail, we define a pad centered coordinate system where y is the above-ground altitude, and x the horizontal distance from the pad. Further, the vehicle inertial coordinate system gives locations along the vehicle axis as measured from the nozzle end. The total height, H , of a Titan IVB vehicle is $H=182.66$ feet. The distance from the nozzle end to the top of the RTG spacecraft, L , is then given by

$$L = H - 31ft \approx 151ft \quad (2-12)$$

With respect to the pad, the vehicle's cg will be denoted (x_{cg}, y_{cg}) , while along the vehicle's axis its center of gravity distance from nozzle end will be denoted by d . Thus, the distance from the cg to SRMU impact point is $(d-10)$, and from the cg to the nose impact point is $(L-d)$. The impact test position of the nose, as a function of time, is then given by

$$\begin{aligned}x(t)_{\text{nose}} &= x(t)_{\text{cg}} - (L-d)\cos(\theta(t)-\theta_e) = x(t)_{\text{cg}} + (L-d)\sin\theta(t) \\y(t)_{\text{nose}} &= y(t)_{\text{cg}} + (L-d)\sin(\theta(t)-\theta_e) = y(t)_{\text{cg}} + (L-d)\cos\theta(t)\end{aligned}\tag{2-13}$$

where $\theta(t)$ is defined in Figure 2-1, and θ_e is the vehicle trajectory elevation angle measured from the horizontal. During the first ten seconds of flight, where our analysis was performed, $\theta_e \approx 90^\circ$, although for accuracy we employ the true value. The equations describing the test position of the tail are similarly written

$$\begin{aligned}x(t)_{\text{tail}} &= x(t)_{\text{cg}} + (d-10)\cos(\theta(t)-\theta_e) = x(t)_{\text{cg}} - (d-10)\sin\theta(t) \\y(t)_{\text{tail}} &= y(t)_{\text{cg}} - (d-10)\sin(\theta(t)-\theta_e) = y(t)_{\text{cg}} - (d-10)\cos\theta(t)\end{aligned}\tag{2-14}$$

Clearly, the test for impact is

$$y(t)_{\text{nose}} < 0 \quad \text{or} \quad y(t)_{\text{tail}} < 0 \quad \text{impact conditions}\tag{2-15}$$

where it is assumed that the ground surrounding the pad is all at the same level.

For this study it was important to know which surface the intact vehicle impact strikes: concrete, sand, or water. Statistics were kept of the number of impacts for each type. To make this determination, we needed to know something about the geometry of the launch pad. At CCAS, the Titan IVB vehicle will launch from Pad 40. This pad, as well as its west coast equivalent, can be modeled as centered on a disk that consists of a fixed ratio of concrete and sand. When an intact vehicle impacts within the disk area, RTGSIM randomly selects the surface type by employing a uniform distribution based on the fixed ratio. Between the disk area and the ocean, the surface is always taken to be sand. This is probably a good approximation since soil acts similarly to sand, as does shallow water which appears in patches near PAD 40. We summarize the specific Titan pad characteristics in Table 2-3.

Table 2-3. Titan Pad Geometry

Feature	Titan IVB Pad 40
Pad to Sand Distance	550 ft
Pad to Water Distance	3000 ft
% Pad Area Concrete	46 %
Pad Shore Angle	-20°
Pad Tower Height	140 ft
Near Tower Distance	10 ft
Far Tower Distance	30 ft

A situation that must be treated separately from ground impact is tower impact. This is a significant event because if the malfunction tumble turn occurs within three seconds after liftoff, the vehicle has a greater chance of striking the tower than the ground. The bottom portion of Table 2-3 presents the tower location and dimensions. We model the tower as occupying the space in a ninety-degree wedge, radially outward from the pad, between the near and far distances given in the table.

3. SUMMARY OF RESULTS

The results of RTGSIM are tabularized in the subsections that follow. This output represents only a small fraction of the total generated. The full set of data was submitted to the 45 SW Safety Office for a more detailed analysis.

The input to RTGSIM consisted of several data files. The Cassini nominal trajectory file was obtained from Lockheed-Martin, and was used with a 93.2° launch azimuth, measured clockwise from the North. The Titan IVB fragment data files were constructed from information supplied by RTI [6]. Each file is organized by fragment group and contains the associated explosion velocity, nominal and $\pm 3\sigma$ ballistic coefficients, consumption rate if a contained segment, propellant weight, and cross sectional area. Vehicle characteristics during a tumble turn, such as center of gravity location and moment of inertia, were obtained from the Lockheed-Martin Titan IVB data book [10].

The initial location of the RTGs and the solid propellant fragments, with respect to the vehicle, is required to accurately predict where the debris will impact in the event of breakup. If breakup does not separate the RTGs from the Cassini spacecraft, the center of mass of each RTG is needed. On the other hand, when there is sufficient explosion pressure to reduce the RTGs into their module components, we employ the center of mass of each of the individual modules. The initial location of each solid propellant fragment is placed at the center of mass of its parent SRMU segment. This approximation follows from the fact that insufficient information is available to determine the true initial location of the propellant fragments. In total, from [8] we extracted the center of mass of each RTG, the RTG modules, and the SRMU segments.

3.1 Intact Vehicle Impacts

The original motivation for this study, was an attempt to reproduce results obtained from a Lockheed-Martin analysis [3]. In particular, their conclusion was that ratio of tail to nose impacts is about 80/20. In their study, L-M computed the vehicle trajectory until its center of gravity reached pad level. Next, they analytically reversed the motion of the vehicle to determine whether the nose or tail struck first. In their study, the launch tower was not present. For their other working conditions, they used the bathtub torque distribution, the nominal MFCO model, and an effective vehicle height of 150 feet.

The results of the first set of runs of RTGSIM are presented in Table 3-1. These were generated using 1,250 Monte Carlo simulations for each tenth of second within the time span (0.1,6.3), for a

total of 78,750 simulations. Beyond five seconds only a few intact impacts were observed, far too few to influence the totals given in the table.

Table 3-1. Initial Nose vs. Tail Results

Case					Nose	Tail
Impact point	Tower impact?	MFCO Model	Torque Distribution	Vehicle Length (ft)		
cg	no	nominal	bathtub	203	38.9% 810	61.1% 1272
true	no	nominal	bathtub	203	51.8% 1859	48.2% 1544
true	yes	nominal	bathtub	203	43.7% 888	56.3% 690
true	yes	nominal	uniform	203	50.0% 1874	50.0% 1873

The first row in Table 3-1 comes closest to the conditions used by L-M. Here, the vehicle height was set to 203 feet due to an erroneous source. Nevertheless, the number of tail impacts is shown to exceed the number of nose impacts by about 50%. Comparing the first two rows highlights an oversight in the L-M study. Since, they flagged the impact when the vehicle cg reached pad level, their study ignored many of the true impact events. These are events that lead to destruction or experience breakup, in the short time between when the nose or tail impacts and the cg impacts. Our results indicate that over 50% of the intact impact events are missed by relying on the cg impact. The third row further shows that half of the total impacts do not strike the ground but the tower. Finally, in the last row, we find that adopting a uniform torque distribution essentially doubles the total number of impacts. This is not surprising since most of the impacts arise from hard-over nozzle deflections.

A set of working conditions were agreed upon for the study appropriate to the Cassini RTG. These were based on a review of the results in Table 3-1, and learning of the appropriate vehicle length to allow (see Section 2.5). This led to a second set of runs that produced the results in Table 3-2. These runs generated 4823 Monte Carlo simulations at every tenth of a second within the time span (0.1,9.9), for a total of 477,477 simulations. The relative proportion of nose to tail impacts given

in the first line seems to agree with the general conclusion of L-M. Again, the exact ratio differs because we flag the true impact and they consider the cg impact.

Table 3-2. Final Nose vs. Tail Results

Case						
Impact point	Tower Impact?	MFCO Model	Torque Distribution	Vehicle Length (ft)	Nose	Tail
true	yes	nominal	uniform	141	26.9% 3116	73.1% 8460
true	yes	upper estimate	uniform	141	38.8% 20816	61.2% 32810

The second row in Table 3-2 shows the sensitivity of the MFCO model to the number of intact impacts. If the MFCO's delay their response to the malfunction by two seconds from nominal performance, the probability of an intact impact increases by a factor of four. Furthermore, such a delay is more likely to result in nose impact, leading to a greater chance of RTG impact followed by the entire intact stack.

Additional results from the second set of runs are given in Table 3-3. This shows more clearly how a small percentage change in the command destruct events can lead to a significant increase in the intact impacts. In any event, there is about a one third chance that the intact impact will strike concrete. Since concrete events must occur within 550 feet of the pad, they are mostly due to the hard-over nozzle deflections. Thus, they are more sensitive to the torque distribution than either sand or water impact.

Table 3-3. Intact Vehicle Impact Statistics

MFCO Model	Event			Surface		
	cd	ads/tower	ground	concrete	sand	water
nominal	75.24%	23.33%	2.42%	35.4% 4100	64.6% 7476	0% 0
upper estimate	60.94%	27.63%	11.23%	26.1% 13992	73.8% 39622	2E-4% 11

To evaluate the risk to the RTG on impact, it is useful to know the impact speed as a function of surface type. In Tables 3-4 and 3-5 we present impact speed histograms for both of the MFCO models. Note that the impact speeds recorded on a concrete surface do not exceed 275 ft/sec. This is reasonable since the vehicle will only impact within this region if its flight time is very short, thus preventing much buildup in speed. Comparison of these tables indicates, again, the dramatic increase in the number of intact impacts by accounting for an additional delay in MFCO reaction time. Note, in particular, that the number of impacts for some of the higher impact speeds has increased by an order of magnitude or more.

Table 3-4. Nominal MFCO Model Impact Speed Histogram

Impact Speed (ft/sec)	Surface		
	concrete	sand	water
0 - 125	0	0	0
125 - 175	2644	3249	0
175 - 225	1428	2540	0
225 - 275	28	1192	0
275 - 325	0	344	0
325 - 375	0	99	0
375 - 425	0	34	0
425 - 475	0	10	0
475 - 525	0	3	0
525 - 575	0	2	0
575 - 625	0	3	0
> 625	0	0	0

Table 3-5. Upper Estimate MFCO Model Impact Speed Histogram

Impact Speed (ft/sec)	Surface		
	concrete	sand	water
0 - 75	0	0	0
75 - 125	1	1	0
125 - 175	8456	11032	0
175 - 225	5444	14987	0
225 - 275	92	8149	0
275 - 325	0	3435	0
325 - 375	0	1378	0
375 - 425	0	428	2
425 - 475	0	148	4
475 - 525	0	45	2
525 - 575	0	19	1
575 - 625	0	2	2
> 625	0	0	0

3.2 Hazard Due to Propellant Explosion Pressure

The focus of this section and the next is to evaluate the hazards that may damage the RTGs or modules sufficiently to expose the radioactive fuel pellets. There are three levels of protection that must be breached for this to occur. First, the plutonium pellets are clad in iridium containment shells. Grouped together in fours, these clads reside in rectangular parallelepiped modules. Finally, each of the three RTGs on the Cassini spacecraft contains eighteen modules. Consequently, vehicle breakup does not necessarily imply any radioactive hazard. Our task is to compute the probabilities of the events where this outcome is possible.

It is generally believed that no vehicle breakup will generate the explosion pressures needed to break open a module and expose any of the internal clads. There are, however, several impact events that

may sufficiently damage a module for this to occur. After breakup, with the module resting on the ground, it may be struck directly by a solid propellant fragment. Above a certain vertical impact speed, the propellant will explode on impact, possibly generating the explosion pressure needed to cause a breach in the module. Actually, the module does not need to be hit directly to experience the necessary pressure. The exploding solid propellant will generate a crater, with an assumed area ten times the cross-sectional area of the propellant fragment. It may be sufficient that the resting module only be within this crater region upon propellant impact for the clads to be exposed.

Similar considerations apply to the RTGs. However, in this case, greater explosion pressures are needed since now both the RTG and its modules must be breached. There are two facts that should be noted at this point. First, the cross-sectional area of an RTG is three times larger than that of a module. Second, there is a far greater probability that an intact RTG will survive the breakup than a module will. Thus, although a direct hit of a module is more likely to create an exposed clad, there is a much larger probability that an RTG will experience the explosion pressure.

RTGSIM was used to perform a Monte Carlo simulation of the breakup and to compute the probabilities of either an RTG or module being struck by a solid propellant fragment, or being inside the crater. In Figure 3-1 we present the event tree employed in determining the final outcome. The numerical values on some of the branches are the conditional probabilities associated with the given events. The sum of the branch conditional probabilities always equals unity. To aid the evaluation of the results, two separate runs were made, thus ignoring the relative probabilities between the two main malfunction modes. The first focused on the on-trajectory malfunction, while the second involved the malfunction tumble turn case.

Considering all possible branches shown in Figure 3-1, there are 23 different fragment cases for which statistics must be kept:

- 1) destroyed right forward SRMU segment
- 2) destroyed left forward SRMU segment
- 3) destroyed right center SRMU segment
- 4) destroyed left center SRMU segment
- 5) destroyed right aft SRMU segment
- 6) destroyed left aft SRMU segment
- 7) rtg #1
- 8) rtg #2
- 9) rtg #3

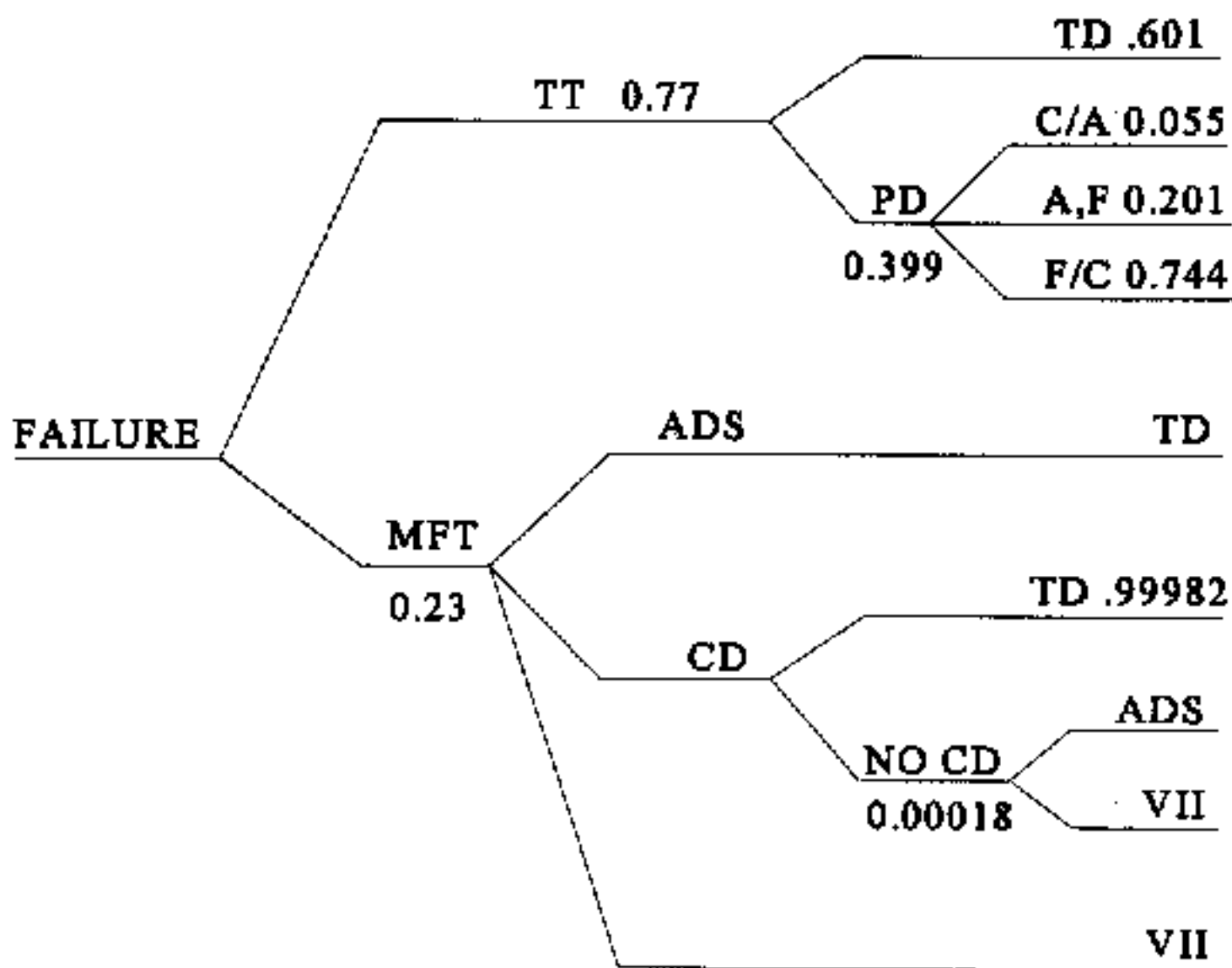


Figure 3-1. Titan IVB SRMU Failure Mode Tree

KEY:

- ADS = Autodestruct System
- C/A = Center/Aft SRMU Segment Assembly
- CD = Command Destruct
- F,A = Forward and Aft Segments
- F/C = Forward/Center SRMU Segment Assembly
- FF = Free-Flying Intact SRMU
- MFT = Malfunction Tumble Turn
- PD = Partial Destruct
- TD = Total Destruct
- TT = Thrust Termination
- VII = Vehicle Intact Impact

- 10) intact right center/aft SRMU segments
- 11) intact left center/aft SRMU segments
- 12) intact right forward SRMU segment
- 13) intact left forward SRMU segment
- 14) intact right aft SRMU segment
- 15) intact left aft SRMU segment
- 16) intact right forward/center SRMU segments
- 17) intact left forward/center SRMU segments
- 18) right nozzle,
- 19) left nozzle
- 20) right dome
- 21) left dome
- 22) intact stack
- 23) tower impact

For each case, except 22 and 23, RTGSIM counts the number of times, N^{hits} , a solid propellant fragment strikes either an RTG or module. A count is also kept of the number of instances where the RTG or module lies in the future crater of the propellant. The probability, P , that one fragment interacts with an RTG or module is then given by

$$P_1 = \frac{N^{hits}}{N^{mc}} \quad (3-1)$$

where N^{mc} is the total number of Monte Carlo simulations performed. For each failure time point, 250000 simulations were run. If a fragment group contains N fragments, then the probability that one or more fragments from that group strike an RTG or module is given by

$$\begin{aligned} P_N &= 1 - (1 - P_1)^N \\ &= 1 - \left(1 - \frac{N^{hits}}{N^{mc}} \right)^N \end{aligned} \quad (3-2)$$

The total probability that an RTG or module is struck by one or more fragments from any group is written

$$\begin{aligned}
 P^{\text{total}} &= 1 - \prod_{i=1}^{N_{\text{cases}}} (1 - P_{N_i}) \\
 &= 1 - \prod_{i=1}^{N_{\text{cases}}} \left(1 - \frac{N_i^{\text{hits}}}{N_i^{\text{no}}} \right)^{N_i}
 \end{aligned}
 \tag{3-3}$$

In Tables 3-6 and 3-7 we present the total probabilities separated into two groups, as a function of failure time. The first group includes every SRMU solid propellant in computing (3-3). The last four columns restrict attention only to fragments that have an impact weight greater than 10000 pounds. The values in these tables verify comments given above. For instance, the probabilities for crater cases are an order of magnitude larger than for direct hits, which agrees with the fact that the crater area is ten times larger. Second the module probabilities are about three times smaller, which is predicted since the module cross-sectional area is one third the RTG area.

Note that these probabilities do not include the mission failure. As long as the probabilities in the tables are much less than 0.1, they can be summed over all failure times for each event. Then, by dividing through by one thousand, one obtains the total mission probability of that event.

In addition to the probabilities, for each fragment case RTGSIM determined the mean impact position and computed the mean impact radius. Records were also kept for the time to impact from breakup, and output as the mean and range values. Similar data was also generated for the impact weights and velocities. We do not present any of these results here, and leave it for the Safety report to distill them.

Table 3-6. Probabilities of RTG Struck by Propellant for Thrust Termination Failures

Failure Time (sec)	All Weights				Weight >10000 lbs			
	RTG Direct	RTG Crater	Module Direct	Module Crater	RTG Direct	RTG Crater	Module Direct	Module Crater
1	1.2E-2	1.0E-1	5.0E-3	4.8E-2	1.2E-2	1.0E-2	5.0E-3	4.8E-2
2	9.4E-3	8.9E-2	4.1E-3	4.2E-2	9.4E-3	8.9E-2	4.1E-3	4.2E-2
3	9.4E-3	8.4E-2	4.1E-3	3.9E-2	9.4E-3	8.4E-2	4.1E-3	3.9E-2
4	7.6E-3	7.4E-2	3.3E-3	3.4E-2	7.6E-3	7.4E-2	3.3E-3	3.4E-2
5	6.9E-3	6.7E-2	3.1E-3	3.1E-2	6.9E-3	6.7E-2	3.1E-3	3.1E-2
6	5.9E-3	5.9E-2	2.7E-3	2.7E-2	5.9E-3	5.9E-2	2.7E-3	2.7E-2
7	5.0E-3	5.3E-2	2.3E-3	2.4E-2	5.0E-3	5.3E-2	2.4E-3	2.4E-2
8	4.5E-3	4.7E-2	2.1E-3	2.1E-2	4.5E-3	4.7E-2	2.1E-3	2.1E-2
9	3.9E-3	4.1E-2	1.8E-3	1.8E-2	3.9E-3	4.1E-2	1.8E-3	1.8E-2
10	3.5E-3	3.6E-2	1.6E-3	1.6E-2	3.5E-3	3.6E-2	1.6E-3	1.6E-2
15	7.6E-4	6.9E-3	7.1E-5	7.6E-4	2.9E-4	2.8E-3	7.1E-5	7.6E-4
20	2.7E-4	3.9E-3	1.1E-6	1.2E-5	1.2E-5	1.1E-4	1.1E-6	1.2E-5

Table 3-7. Probabilities of RTG Struck by Propellant for Tumble Turn Failures

Failure Time (sec)	All Weights				Weight >10000 lbs			
	RTG Direct	RTG Crater	Module Direct	Module Crater	RTG Direct	RTG Crater	Module Direct	Module Crater
1	2.3E-2	2.1E-1	1.3E-3	1.3E-2	3.5E-3	3.6E-2	3.1E-4	3.3E-3
2	1.8E-2	1.7E-1	1.1E-3	1.1E-2	2.2E-3	2.3E-2	3.1E-4	2.9E-3
3	1.4E-2	1.3E-1	1.0E-3	9.7E-3	1.6E-3	1.6E-2	3.2E-4	3.1E-3
4	1.3E-2	1.3E-1	1.1E-3	1.2E-2	1.8E-3	1.7E-2	4.0E-4	4.2E-3
5	7.4E-3	8.1E-2	6.8E-4	6.4E-3	1.3E-3	1.3E-2	1.7E-4	1.8E-3
6	5.7E-3	5.8E-2	2.5E-4	2.8E-3	1.2E-3	1.1E-2	5.4E-5	5.6E-4
7	4.9E-3	4.3E-2	1.4E-4	1.5E-3	8.4E-4	7.9E-3	2.3E-5	2.7E-4
8	3.0E-3	3.0E-2	6.6E-5	6.2E-4	2.6E-4	2.2E-3	1.5E-5	1.5E-4
9	1.9E-3	1.9E-2	5.1E-5	4.7E-4	1.3E-4	1.1E-3	1.0E-5	1.1E-4
10	2.7E-3	2.1E-2	2.8E-5	3.4E-4	6.3E-5	6.9E-4	5.7E-6	6.9E-5

3.3 Hazard Due to Heat Transfer

In the last subsection, we presented results that relate to a brute force approach to exposing the Plutonium pellets. This involves the application of a pressure wave originating from an exploding fragment of solid propellant. In this situation, the breach of the iridium shell would occur almost instantaneously. If the clads are not damaged after all the fragments have impacted, a second danger then arises that has the potential to be just as harmful.

After the RTGs or modules have impacted and are at rest, they may be surrounded by one or more burning solid propellant fragments. These fragments may burn on the order of ten minutes or more. This creates a situation where the iridium shell may be melted off the pellets. Factors that are important in deciding whether this occurs, are the number of fragments near the RTGs and modules, and their distance. Consequently, RTGSIM was coded to generate this type of output for the Monte Carlo simulations generated for the last subsection. The results are presented on the next few pages in Tables 3-8 through 3-11.

Since large solid propellant fragments burn longer and generate more heat, each table indicates the number of fragments more than 10000 pounds. These fragments generally represent intact SRMU segments at breakup. The greatest danger is from burning propellant within just a few feet of the iridium casing. However, several larger fragments within 30 feet may still pose a danger, depending on how much damage had been previously done from the explosive pressure. For these reasons, we were asked to generate the average number of fragments impacting within 3, 10, and 30 feet from the RTGs and modules.

For the on-trajectory malfunction, Tables 3-8 and 3-9 show that most of the fragments that impact near the RTGs and modules are due to the SRMU segments. This is not surprising because, except for the forward segment, the intact segments have no effective explosion velocity. They impact directly under the breakup position, which is where the RTGs and modules are also most likely to concentrate. These results may, therefore, be very sensitive to the explosion velocity model of the intact segments, RTGs, and modules.

For tumble turn malfunctions, Tables 3-10 and 3-11 show that there is only a small probability for any fragment to land very close to the RTGs or modules. Furthermore, it appears quite unlikely that any of the intact SRMUs will pose any threat to the pellets. In general, the tumble turn events generate far fewer fragment neighbors than the thrust termination cases. However, this does not really ease the concern because, as shown in the fault tree in Figure 3-1, the tumble turn failure will occur fewer than one in four malfunctions.

Finally, in Tables 3-12 and 3-13, we present the probability for an RTG or module to overlap a solid propellant fragment, or the corresponding crater. The events associated with these probabilities differ from those in Tables 3-7 and 3-8 in that, here, it does not matter which item struck the ground first. Thus, the probabilities in Tables 3-12 and 3-13 not only include the events represented by tables 3-7 and 3-8, but also those where the RTG or module strikes the propellant fragment. Consequently, the values in these final tables may be larger by an order of magnitude or more.

Table 3-8. Average Number of Fragment Impacts Near RTG for Thrust Termination Failure

Failure Time (sec)	All Weights			Weight > 10000 lbs		
	< 3 ft	< 10 ft	< 30 ft	< 3 ft	< 10 ft	< 30 ft
1	0.34	2.34	9.15	0.13	1.12	2.50
2	0.29	2.01	7.10	0.13	1.10	2.40
3	0.26	1.80	5.78	0.13	1.09	2.34
4	0.23	1.60	4.87	0.14	1.07	2.28
5	0.22	1.48	4.29	0.15	1.05	2.25
6	0.22	1.40	3.90	0.15	1.04	2.23
7	0.21	1.33	3.65	0.16	1.02	2.20
8	0.21	1.27	3.40	0.17	1.01	2.19
9	0.21	1.23	3.25	0.17	1.00	2.17
10	0.21	1.19	3.12	0.17	0.98	2.15
15	0.011	0.066	0.655	0.001	0.003	0.168
20	0.003	0.021	0.137	0.000	0.000	0.002

Table 3-9. Average Number of Fragment Impact Near Modules for Thrust Termination Failure

Failure Time (sec)	All Weights			Weight > 10000 lbs		
	< 3 ft	< 10 ft	< 30 ft	< 3 ft	< 10 ft	< 30 ft
1	0.15	1.43	8.55	0.06	0.61	2.46
2	0.13	1.21	6.69	0.06	0.60	2.37
3	0.12	1.08	5.48	0.06	0.60	2.30
4	0.11	0.96	4.62	0.07	0.59	2.25
5	0.11	0.87	4.07	0.07	0.59	2.21
6	0.11	0.83	3.71	0.08	0.59	2.17
7	0.11	0.79	3.45	0.08	0.59	2.14
8	0.10	0.75	3.22	0.08	0.58	2.12
9	0.10	0.74	3.09	0.08	0.58	2.10
10	0.10	0.72	2.97	0.09	0.59	2.09
15	0.002	0.020	0.185	0.000	0.001	0.008
20	0.002	0.012	0.103	0.000	0.000	0.002

Table 3-10. Average Number of Fragment Impacts Near RTG for Tumble Turn Failures

Failure Time (sec)	All Weights			Weight > 10000 lbs		
	< 3 ft	< 10 ft	< 30 ft	< 3 ft	< 10 ft	< 30 ft
1	0.13	0.66	4.61	0.01	0.05	0.22
2	0.34	1.77	11.77	0.02	0.07	0.32
3	0.25	1.31	8.86	0.01	0.06	0.29
4	0.20	1.07	7.30	0.02	0.07	0.28
5	0.15	0.74	4.73	0.01	0.05	0.21
6	0.10	0.49	3.14	0.01	0.04	0.17
7	0.07	0.35	2.25	0.01	0.04	0.15
8	0.05	0.28	1.76	0.01	0.03	0.13
9	0.04	0.22	1.36	0.01	0.03	0.12
10	0.04	0.19	1.16	0.01	0.03	0.11

Table 3-11. Average Number of Fragment Impacts Near Modules for Tumble Turn Failures

Failure Time (sec)	All Weights			Weight > 10000 lbs		
	< 3 ft	< 10 ft	< 30 ft	< 3 ft	< 10 ft	< 30 ft
1	0.04	0.37	3.21	0.00	0.02	0.10
2	0.10	0.86	7.14	0.01	0.04	0.22
3	0.10	0.81	6.57	0.01	0.04	0.20
4	0.09	0.69	5.51	0.01	0.04	0.21
5	0.05	0.42	3.31	0.01	0.03	0.15
6	0.03	0.27	2.15	0.01	0.03	0.12
7	0.03	0.21	1.59	0.01	0.02	0.11
8	0.02	0.15	1.13	0.00	0.02	0.08
9	0.01	0.10	0.79	0.00	0.01	0.03
10	0.01	0.07	0.62	0.00	0.00	0.02

Table 3-12. Probabilities of RTG Coincident with Propellant for Thrust Termination Failure

Failure Time (sec)	All Weights				Weight > 10000 lbs			
	RTG Direct	RTG Crater	Module Direct	Module Crater	RTG Direct	RTG Crater	Module Direct	Module Crater
1	0.06	0.88	0.02	0.29	0.02	0.81	0.01	0.26
2	0.06	0.86	0.02	0.29	0.02	0.81	0.01	0.27
3	0.05	0.85	0.02	0.29	0.02	0.80	0.02	0.27
4	0.04	0.84	0.02	0.29	0.03	0.80	0.02	0.28
5	0.04	0.83	0.02	0.30	0.03	0.80	0.02	0.29
6	0.05	0.82	0.02	0.30	0.03	0.79	0.02	0.29
7	0.05	0.81	0.02	0.30	0.04	0.79	0.02	0.30
8	0.05	0.80	0.02	0.31	0.04	0.78	0.02	0.30
9	0.05	0.79	0.02	0.31	0.05	0.78	0.02	0.30
10	0.05	0.79	0.02	0.32	0.05	0.77	0.02	0.32
15	2.1E-3	2.5E-2	1.4E-4	1.8E-3	3.5E-4	4.0E-3	8.4E-5	9.1E-4
20	5.9E-4	7.2E-3	8.6E-5	8.1E-4	3.1E-5	3.1E-4	1.7E-5	1.6E-4

Table 3-13. Probabilities of RTG Coincident with Propellant for Tumble Turn Failures

Failure Time (sec)	All Weight				Weight > 10000 lbs			
	RTG Direct	RTG Crater	Module Direct	Module Crater	RTG Direct	RTG Crater	Module Direct	Module Crater
1	2.9E-2	2.5E-1	2.5E-3	2.4E-2	5.6E-3	5.6E-2	1.0E-3	1.1E-2
2	7.1E-2	5.2E-1	5.7E-3	5.8E-2	6.0E-3	6.2E-2	1.9E-3	1.9E-2
3	5.1E-2	4.2E-1	5.4E-3	5.2E-2	5.4E-3	5.6E-2	1.7E-3	1.8E-2
4	4.2E-2	3.7E-1	5.0E-3	5.1E-2	6.6E-3	6.3E-2	2.1E-3	2.1E-2
5	3.0E-2	2.8E-1	3.6E-3	3.6E-2	5.1E-3	5.0E-2	1.6E-3	1.6E-2
6	2.5E-2	2.0E-1	2.5E-3	2.5E-2	4.7E-3	4.4E-2	1.4E-3	1.4E-2
7	1.5E-2	1.5E-1	2.2E-3	2.2E-2	4.1E-3	3.9E-2	1.3E-3	1.3E-2
8	1.2E-2	1.2E-1	1.7E-3	1.7E-2	3.7E-3	3.5E-2	1.2E-3	1.1E-2
9	1.0E-2	9.8E-2	7.5E-4	7.4E-3	3.4E-3	3.4E-2	3.4E-4	3.5E-3
10	1.0E-2	9.3E-2	5.4E-4	5.0E-3	3.5E-3	3.3E-2	2.1E-4	2.1E-3

4. REFERENCES

- [1] Wilde, P., et al., FY96 BLASTX/C Development Activities, Report No. 96-326/84-02, ACTA Inc., Torrance, CA, September 1996.
- [2] Salerno, C. L., Launch Vehicle Simulation Data Book. Titan IV/Centaur Configuration Type II, CRDL Item No. 072A2, Martin Marietta Technologies, Inc., Space Launch Systems, Denver CO., June 1995.
- [3] Rudolph, L. K., Titan IV/Cassini Full Stack Intact Impact (FSII) Trajectory Analysis, Cassini RTG-238, Lockheed-Martin Astronautics, Memorandum, August 2, 1996.
- [4] Frank, M., Review of Flight Control Officer Response Curves and Suggested Alternatives, Safety Factor Associates Inc., January 1996.
- [5] Frank, M., Upper Estimate, Memorandum, Safety Factor Associates Inc., October 1996.
- [6] Weaver, J. R., Ward J. A., and Laney R. T., Titan IV Fragmentation Model, RTI Report No. RTI/5180/60-33F, September 1995.
- [7] Weaver, J. R., Imparted Velocities for Intact SRMU Segments, Memorandum, RTI, December 1996.
- [8] Rudolph, L. K., Cassini Titan IV/Centaur RTG Safety Data Book, Rev. A, Report No. NAS3-00031, Lockheed-Martin Astronautics, June 1996.
- [9] McRonald, A., Average Distance of Large SRMU Fragments Exploding Upon Ground Impact from the RTGs, Report No. 312/95.6-806, Memorandum, Jet Propulsion Laboratory, October 1995.
- [10] Salerno, C. L., Launch Vehicle Simulation Data Book: Titan IV/Centaur Configuration Type II, CRDL Item no. 072A2, Lockheed-Martin, Space Launch Systems, Denver, CO, June 1995.